EURASIP Journal on Wireless Communications and Networking 2005:2, 163–174

A Low-Complexity KL Expansion-Based Channel Estimator for OFDM Systems

Habib Şenol
Department of Computer Engineering, Kadir Has University, Cibali 34230, Istanbul, Turkey
Email: hsenol@khas.edu.tr

Hakan A. Çırpan
Department of Electrical-Electronics Engineering, Istanbul University, Avcilar 34850, Istanbul, Turkey
Email: hcirpan@istanbul.edu.tr

Erdal Panayırcı
Department of Electronics Enginering, IŞik University, Maslak 80670, Istanbul, Turkey
Email: eepanay@isikun.edu.tr

Received 23 April 2004; Revised 18 October 2004

This paper first proposes a computationally efficient, pilot-aided linear minimum mean square error (MMSE) batch channel estimation algorithm for OFDM systems in unknown wireless fading channels. The proposed approach employs a convenient representation of the discrete multipath fading channel based on the Karhunen-Loeve (KL) orthogonal expansion and finds MMSE estimates of the uncorrelated KL series expansion coefficients. Based on such an expansion, no matrix inversion is required in the proposed MMSE estimator. Moreover, optimal rank reduction is achieved by exploiting the optimal truncation property of the KL expansion resulting in a smaller computational load on the estimation algorithm. The performance of the proposed approach is studied through analytical and experimental results. We then consider the stochastic Cramér-Rao bound and derive the closed-form expression for the random KL coefficients and consequently exploit the performance of the MMSE channel estimator based on the evaluation of minimum Bayesian MSE. We also analyze the effect of a modelling mismatch on the estimator performance. To further reduce the complexity, we extend the batch linear MMSE to the sequential linear MMSE estimator. With the fast convergence property and the simple structure, the sequential linear MMSE estimator provides an attractive alternative to the implementation of channel estimator.

Keywords and phrases: channel estimation, OFDM systems, MMSE estimation.

1. INTRODUCTION

With unprecedented demands on bandwidth due to the explosive growth of broadband wireless services usage, there is an acute need for a high-rate and bandwidth-efficient digital transmission. In response to this need, the research community has been extensively investigating efficient schemes that make efficient utilization of the limited bandwidth and cope with the adverse access environments [1]. These access environments may create different channel impairments and dictate unique sets of advanced signal processing algorithms to combat specific impairments.

Multicarrier (MC) transmission scheme, especially orthogonal frequency-division multiplexing (OFDM), has recently attracted considerable attention since it has been shown to be an effective technique to combat delay spread or frequency-selective fading of wireless or wireline channels, thereby improving the capacity and enhancing the performance of transmission. This approach has been adopted as the standard in several outdoor and indoor high-speed wireless and wireline data applications, including terrestrial digital broadcasting (DAB and DVB) in Europe, and high-speed modems over digital subscriber lines in the US. It has also been implemented for broadband indoor wireless systems including IEEE802.11a, MMAC, and HIPERLAN/2.

An OFDM system operating over a frequency-selective wireless communication channel effectively forms a number of parallel frequency-nonselective fading channels, thereby

reducing intersymbol interference (ISI) and obviating the need for complex equalization, thus greatly simplifying channel estimation/equalization task. Moreover, OFDM is bandwidth efficient since the spectra of the neighboring subchannels overlap, yet channels can still be separated through the use of orthogonality of the carriers. Furthermore, its structure also allows efficient hardware implementations using fast Fourier transform (FFT) and polyphase filtering [2].

Although the structure of OFDM signalling avoids ISI arising due to channel memory, fading multipath channel still introduces random attenuations on each tone. Furthermore, simple frequency-domain equalization, which divides the FFT output by the corresponding channel frequency response, does not assure symbol recovery if the channel has nulls on some subcarriers. Hence, advanced signal processing algorithms have to be used for accurate channel estimation to improve the performance of the OFDM systems. Numerous pilot-aided channel estimation methods for OFDM have been developed [3, 4, 5, 6]. In particular, a low-rank approximation is applied to linear MMSE estimator for the estimation of subcarrier channel attenuations by using the frequency correlation of the channel [3]. Two pilot-aided MLE and MMSE schemes are revisited and compared in terms of computational complexity in [4]. In [5], an MMSE channel estimator, which makes full use of the time and frequency correlation of the time-varying dispersive channel, was proposed. Moreover, low-complexity MMSE doubly channel estimation approaches were presented in [6] based on embedding Kronecker-delta pilot sequences.

Multipath fading channels have been studied extensively, and several models have been developed to describe their variations [7]. In many cases, the channel taps are modelled as general lowpass stochastic processes (e.g., [8]), the statistics depend on mobility parameters. A different approach explicitly models the multipath channel taps by the Karhunen-Loeve (KL) series representation [9]. KL expansion models have also been used previously in modelling the multipath channel within a CDMA scenario [10]. In the case of KL series representation of stochastic process, a convenient choice of orthogonal basis set is one that makes the expansion coefficient random variables uncorrelated. When these orthogonal bases are employed to expand the channel taps of the multipath channel, uncorrelated coefficients indeed represent the multipath channel. Therefore, KL representation allows one to tackle the estimation of correlated multipath parameters as a parameter estimation problem of the uncorrelated coefficients. Exploiting KL expansion, the main contribution of this paper is to propose a computationally efficient, pilot-aided MMSE channel estimation algorithm. Based on such representation, no matrix inversion is required in the proposed batch approach. Moreover, optimal rank reduction is achieved by exploiting the optimal truncation property of the KL expansion resulting in a smaller computational load on the estimation algorithm. The performance of the proposed batch approach is explored based on the evaluation of the stochastic Cramér-Rao bound for the random KL coefficients. We also analyze the effect of a modelling mismatch on the estimator performance. In contrast to [3], the proposed batch approach employs KL expansion of multipath channel parameters and reduces the complexity of the singular value decomposition (SVD) used in *eigendecomposition* by estimating multipath channel parameters instead of channel attenuations on each tone. In addition, we propose the simple sequential MMSE implementation for the estimation of the KL expansion coefficients, which does not require to perform matrix inversion as well.

The rest of the paper is organized as follows. Section 2 describes a general model for OFDM systems and briefly introduces the channel estimation task. Section 3 derives a basic and simplified approach to MMSE batch channel estimation for OFDM systems. To show its efficiency, the performance bounds are analyzed and the performance degradation due to a mismatch of the estimator to the channel statistics as well as the SNR is demonstrated. The sequential MMSE estimator is introduced in Section 4 and its convergence behavior is also analyzed. Some simulation examples are provided in Section 5. Finally, conclusions are drawn in Section 6.

2. SYSTEM MODEL

In order to eliminate ISI arising due to multipath channel and preserve orthogonality of the subcarrier frequencies (tones), conventional OFDM systems first take the IFFT of data symbols and then insert redundancy in the form of a cyclic prefix (CP) of length L_{CP} larger than the channel order L. CP is discarded at the receiver and the remaining part of the OFDM symbol is FFT processed. Combination of IFFT and CP at the transmitter with the FFT at the receiver divides the frequency-selective channel into several separate flat-fading subchannels. The block diagram in Figure 1 describes the conventional OFDM system. We consider an OFDM system with K subcarriers for the transmission of K parallel data symbols. Thus, the information stream $X(n)$ is parsed into K-long blocks: $\mathbf{X}_i = [X_i(0), X_i(1), \ldots, X_i(K-1)]^T$, where $i = 1, 2, \ldots$ is the block index and the superscript $(\cdot)^T$ indicates the vector transpose. The $K \times 1$ symbol block is then mapped to a $(K+L) \times 1$ vector by first taking the IFFT of $\mathbf{X}_i$ and then replicating the last L_{CP} elements as

$$\mathbf{s}_i = \left[s_i(0), s_i(1), \ldots, s_i\left(K + L_{\mathrm{CP}} - 1\right)\right]^T. \tag{1}$$

$\mathbf{s}_i$ is serially transmitted over the channel. At the receiver, the CP of length L_{CP} is removed first and FFT is performed on the remaining $K \times 1$ vector. Therefore, we can write the output of the FFT unit in matrix form as

$$\mathbf{Y}_i = \mathbf{A}_i \mathbf{H}_i + \boldsymbol{\eta}_i, \tag{2}$$

where $\mathbf{A}_i$ is the diagonal matrix $\mathbf{A}_i = \mathrm{diag}(\mathbf{X}_i)$ and $\mathbf{H}_i$ is the channel vector. The elements of $\mathbf{H}_i$ are the values of the channel frequency response evaluated at the subcarriers. Therefore, we can write $\mathbf{H}_i = [H_i(0), H_i \exp(j2\pi/K), \ldots, H_i \exp(j2\pi(K-1)/K)]^T$ as $\mathbf{H}_i = \mathcal{F}\mathbf{h}_i$, where $\mathcal{F}$ is the FFT matrix with (m,n) entry $\exp(-j2\pi mn/K)$ and $\mathbf{h}_i = [h_i(0), h_i(1), \ldots, h_i(L-1)]^T$. $\mathbf{h}_i$ modelled as a complex Gaussian vector with $\mathbf{h}_i \sim \mathcal{N}(\mathbf{0}, \mathbf{C}_{\mathbf{h}_i})$ represents the overall

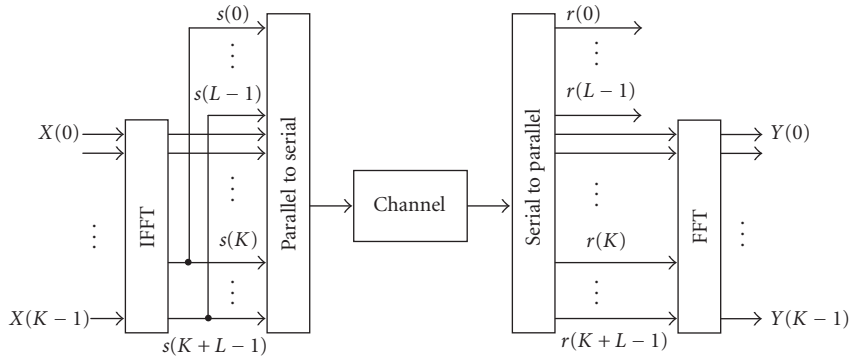

Figure 1: OFDM system block diagram.

channel impulse during the ith OFDM block. Finally, $\boldsymbol{\eta}_i$ is a $K \times 1$ zero-mean, i.i.d. complex Gaussian vector that models additive noise in the K subchannels (tones). We have $E[\boldsymbol{\eta}_i \boldsymbol{\eta}_i^\dagger] = \sigma^2 \mathbf{I}_K$ where $\mathbf{I}_K$ represents a $K \times K$ identity matrix, σ^2 is the variance of the additive noise entering the system, and the superscript $(\cdot)^\dagger$ indicates the Hermitian transpose.

Based on model (2), our main objective in this paper is to develop both batch and sequential pilot-aided channel estimation algorithm according to MMSE criterion and then explore the performance of the estimators. A batch approach adapted herein explicitly models the channel parameters by the KL series representation and estimates the uncorrelated expansion coefficients. Furthermore, the computational load of the proposed MMSE estimation technique is further reduced with the application of the KL expansion optimal truncation property [9]. We then introduce batch channel MMSE approach first.

3. MMSE ESTIMATION OF KL COEFFICIENTS: BATCH APPROACH

A low-rank approximation to the frequency-domain linear MMSE channel estimator is provided by [3] to reduce the complexity of the estimator. Optimal rank reduction is achieved in this approach by using the SVD of the channel attenuations covariance matrix $\mathbf{C_H}$ of dimension $K \times K$. In contrast, we adopt the MMSE estimator for the estimation of multipath channel parameter $\mathbf{h}$ that uses covariance matrix of dimension $L \times L$. The proposed approach employs KL expansion of multipath channel parameters and reduces the complexity of the SVD used in *eigendecomposition* since L is usually much less than K. We will now develop MMSE batch estimator for pilot-assisted OFDM system in the sequel.

3.1. MMSE channel estimation

Pilot-symbol-assisted techniques can provide information about an undersampled version of the channel that may be easier to identify. In this paper, we therefore address the problem of estimating multipath channel parameters by exploiting the distributed training symbols. Considering (2), and in order for the pilot symbols to be included in the output vector for our estimation purposes, we focus on an undersampled signal model. Assuming that K_p pilot symbols are uniformly inserted at known locations of the ith OFDM block, the $K_p \times 1$ vector corresponding to the FFT output at the pilot locations becomes

$$\mathbf{Y} = \mathbf{AFh} + \boldsymbol{\eta}, \tag{3}$$

where $\mathbf{A} = \mathrm{diag}[\mathbf{A}_i(0), \mathbf{A}_i(\Delta), \ldots, \mathbf{A}_i((K_p - 1)\Delta)]$ is a diagonal matrix with pilot-symbol entries, Δ is pilot spacing interval, $\mathbf{F}$ is a $K_p \times L$ FFT matrix generated based on pilot indices, and similarly $\boldsymbol{\eta}$ is the undersampled noise vector.

For the estimation of $\mathbf{h}$, the new linear signal model can be formed by premultiplying both sides of (3) by $\mathbf{A}^\dagger$ and assuming that pilot symbols are taken from a PSK constellation $\mathbf{A}^\dagger \mathbf{A} = \mathbf{I}_{K_p}$, then the new form of (3) becomes

$$\begin{aligned} \mathbf{A}^\dagger \mathbf{Y} &= \mathbf{Fh} + \mathbf{A}^\dagger \boldsymbol{\eta}, \\ \widetilde{\mathbf{Y}} &= \mathbf{Fh} + \widetilde{\boldsymbol{\eta}}, \end{aligned} \tag{4}$$

where $\widetilde{\mathbf{Y}}$ and $\widetilde{\boldsymbol{\eta}}$ are related to $\mathbf{Y}$ and $\boldsymbol{\eta}$ by the linear transformation, respectively. Furthermore, $\widetilde{\boldsymbol{\eta}}$ is statistically equivalent to $\boldsymbol{\eta}$.

Equation (4) offers a Bayesian linear model representation. Based on this representation, the minimum variance estimator for the time-domain channel vector $\mathbf{h}$ for the ith OFDM block, that is, conditional mean of $\mathbf{h}$ given $\widetilde{\mathbf{Y}}$, can be obtained using MMSE estimator. We should clearly make the assumptions that $\mathbf{h} \sim \mathcal{N}(\mathbf{0}, \mathbf{C_h})$, $\widetilde{\boldsymbol{\eta}} \sim \mathcal{N}(\mathbf{0}, \mathbf{C}_{\widetilde{\eta}})$, and $\mathbf{h}$ is uncorrelated with $\widetilde{\boldsymbol{\eta}}$. Therefore, MMSE estimate of $\mathbf{h}$ is given by [11]

$$\widehat{\mathbf{h}} = \left(\mathbf{F}^\dagger \mathbf{C}_{\widetilde{\eta}}^{-1} \mathbf{F} + \mathbf{C}_{\mathbf{h}}^{-1}\right)^{-1} \mathbf{F}^\dagger \mathbf{C}_{\widetilde{\eta}}^{-1} \widetilde{\mathbf{Y}}. \tag{5}$$

Due to PSK pilot-symbol assumption together with the result $\mathbf{C}_{\widetilde{\eta}} = E[\widetilde{\boldsymbol{\eta}} \widetilde{\boldsymbol{\eta}}^\dagger] = \sigma^2 \mathbf{I}_{K_p}$, we can therefore express (5) by

$$\widehat{\mathbf{h}} = \left(\mathbf{F}^\dagger \mathbf{F} + \sigma^2 \mathbf{C}_{\mathbf{h}}^{-1}\right)^{-1} \mathbf{F}^\dagger \widetilde{\mathbf{Y}}. \tag{6}$$

Under the assumption that uniformly spaced pilot symbols are inserted with pilot spacing interval Δ and $K = \Delta \times K_p$, correspondingly, $\mathbf{F}^\dagger \mathbf{F}$ reduces to $\mathbf{F}^\dagger \mathbf{F} = K_p \mathbf{I}_L$. Then according to (6) and $\mathbf{F}^\dagger \mathbf{F} = K_p \mathbf{I}_L$, we arrive at the expression

$$\widehat{\mathbf{h}} = \left(K_p \mathbf{I}_L + \sigma^2 \mathbf{C}_{\mathbf{h}}^{-1}\right)^{-1} \mathbf{F}^\dagger \widetilde{\mathbf{Y}}. \tag{7}$$

Since MMSE estimation still requires the inversion of $\mathbf{C}_\mathbf{h}^{-1}$, it therefore suffers from a high computational complexity. However, it is possible to reduce the complexity of the MMSE algorithm by diagonalizing channel covariance matrix with a KL expansion.

3.2. KL expansion

Channel impulse response $\mathbf{h}$ is a zero-mean Gaussian process with covariance matrix $\mathbf{C}_\mathbf{h}$. The KL transformation is therefore employed here to rotate the vector $\mathbf{h}$ so that all its components are uncorrelated. The vector $\mathbf{h}$, representing the channel impulse response during ith OFDM block, can be expressed as a linear combination of the orthonormal basis vectors as follows:

$$\mathbf{h} = \sum_{l=0}^{L-1} g_l \boldsymbol{\psi}_l = \boldsymbol{\Psi}\mathbf{g}, \tag{8}$$

where $\boldsymbol{\Psi} = [\boldsymbol{\psi}_0, \boldsymbol{\psi}_1, \ldots, \boldsymbol{\psi}_{L-1}]$, $\boldsymbol{\psi}_i$'s are the orthonormal basis vectors, $\mathbf{g} = [g_0, g_1, \ldots, g_{L-1}]^T$, and g_l's are the weights of the expansion. If we form the covariance matrix $\mathbf{C}_\mathbf{h}$ as

$$\mathbf{C}_\mathbf{h} = \boldsymbol{\Psi}\boldsymbol{\Lambda}_\mathbf{g}\boldsymbol{\Psi}^\dagger, \tag{9}$$

where $\boldsymbol{\Lambda}_\mathbf{g} = E\{\mathbf{g}\mathbf{g}^\dagger\}$, the KL expansion is the one in which $\boldsymbol{\Lambda}_\mathbf{g}$ of $\mathbf{C}_\mathbf{h}$ is a diagonal matrix (i.e., the coefficients are uncorrelated). If $\boldsymbol{\Lambda}_\mathbf{g}$ is diagonal, then the form $\boldsymbol{\Psi}\boldsymbol{\Lambda}_\mathbf{g}\boldsymbol{\Psi}^\dagger$ is called an *eigendecomposition* of $\mathbf{C}_\mathbf{h}$. The fact that only the eigenvectors diagonalize $\mathbf{C}_\mathbf{h}$ leads to the desirable property that the KL coefficients are uncorrelated. Furthermore, in the Gaussian case, the uncorrelatedness of the coefficients renders them independent as well, providing additional simplicity.

Thus, the channel estimation problem in this application is equivalent to estimating the i.i.d. complex Gaussian vector $\mathbf{g}$ KL expansion coefficients.

3.3. Estimation of KL coefficients

In contrast to (4) in which only $\mathbf{h}$ is to be estimated, we now assume that the KL coefficient vector $\mathbf{g}$ is unknown. Thus the data model (4) is rewritten for each OFDM block as

$$\widetilde{\mathbf{Y}} = \mathbf{F}\boldsymbol{\Psi}\mathbf{g} + \widetilde{\boldsymbol{\eta}} \tag{10}$$

which is also recognized as a Bayesian linear model, and recall that $\mathbf{g} \sim \mathcal{N}(\mathbf{0}, \boldsymbol{\Lambda}_\mathbf{g})$. As a result, the MMSE estimator of $\mathbf{g}$ is

$$\begin{aligned}\hat{\mathbf{g}} &= \boldsymbol{\Lambda}_\mathbf{g}\left(K_p\boldsymbol{\Lambda}_\mathbf{g} + \sigma^2\mathbf{I}_L\right)^{-1}\boldsymbol{\Psi}^\dagger\mathbf{F}^\dagger\widetilde{\mathbf{Y}} \\ &= \boldsymbol{\Gamma}\boldsymbol{\Psi}^\dagger\mathbf{F}^\dagger\widetilde{\mathbf{Y}},\end{aligned} \tag{11}$$

where

$$\begin{aligned}\boldsymbol{\Gamma} &= \boldsymbol{\Lambda}_\mathbf{g}\left(K_p\boldsymbol{\Lambda}_\mathbf{g} + \sigma^2\mathbf{I}_L\right)^{-1} \\ &= \operatorname{diag}\left\{\frac{\lambda_{g_0}}{\lambda_{g_0}K_p + \sigma^2}, \ldots, \frac{\lambda_{g_{L-1}}}{\lambda_{g_{L-1}}K_p + \sigma^2}\right\}\end{aligned} \tag{12}$$

and $\lambda_{g_0}, \lambda_{g_1}, \ldots, \lambda_{g_{L-1}}$ are the singular values of $\boldsymbol{\Lambda}_\mathbf{g}$.

It is clear that the complexity of the MMSE estimator in (7) is reduced by the application of KL expansion. However, the complexity of $\hat{\mathbf{g}}$ can be further reduced by exploiting the optimal truncation property of the KL expansion [9]. MMSE estimator of $\mathbf{g}$ requires $4L^2 + 4LK_p + 2L$ real multiplications. From the results presented in [4], ML estimator of $\mathbf{g}$ is obtained as follows:

$$\hat{\mathbf{g}} = \frac{1}{K_p}\boldsymbol{\Psi}^\dagger\mathbf{F}^\dagger\widetilde{\mathbf{Y}}. \tag{13}$$

Note that, according to (13), the ML estimator of $\mathbf{g}$ requires $4L^2 + 4LK_p$ real multiplications.

3.4. Truncated KL expansion

A truncated expansion $\mathbf{g}_r$ can be formed by selecting r orthonormal basis vectors among all basis vectors that satisfy $\mathbf{C}_\mathbf{h}\boldsymbol{\Psi} = \boldsymbol{\Psi}\boldsymbol{\Lambda}_\mathbf{g}$. The optimal one that yields the smallest average mean squared truncation error $(1/L)E[\boldsymbol{\epsilon}_r^\dagger\boldsymbol{\epsilon}_r]$ is the one expanded with the orthonormal basis vectors associated with the first largest r eigenvalues as given by

$$\frac{1}{L}E[\boldsymbol{\epsilon}_r^\dagger\boldsymbol{\epsilon}_r] = \frac{1}{L}\sum_{i=r}^{L-1}\lambda_{g_i}, \tag{14}$$

where $\boldsymbol{\epsilon}_r = \mathbf{g} - \mathbf{g}_r$. For the problem at hand, truncation property of the KL expansion results in a low-rank approximation as well. Thus, a rank-r approximation to $\boldsymbol{\Lambda}_{\mathbf{g}_r}$ is defined as

$$\boldsymbol{\Lambda}_{\mathbf{g}_r} = \operatorname{diag}\{\lambda_{g_0}, \lambda_{g_1}, \ldots, \lambda_{g_{r-1}}, 0, \ldots, 0\}. \tag{15}$$

Since the trailing $L-r$ variances $\{\lambda_{g_l}\}_{l=r}^{L-1}$ are small compared to the leading r variances $\{\lambda_{g_l}\}_{l=0}^{r-1}$, then the trailing $L-r$ variances are set to zero to produce the approximation. However, typically the pattern of eigenvalues for $\boldsymbol{\Lambda}_\mathbf{g}$ splits the eigenvectors into dominant and subdominant sets. Then the choice of r is more or less obvious. The optimal truncated KL (rank-r) estimator of (11) now becomes

$$\hat{\mathbf{g}}_r = \boldsymbol{\Gamma}_r\boldsymbol{\Psi}^\dagger\mathbf{F}^\dagger\widetilde{\mathbf{Y}}, \tag{16}$$

where

$$\begin{aligned}\boldsymbol{\Gamma}_r &= \boldsymbol{\Lambda}_{\mathbf{g}_r}\left(K_p\boldsymbol{\Lambda}_{\mathbf{g}_r} + \sigma^2\mathbf{I}_L\right)^{-1} \\ &= \operatorname{diag}\left\{\frac{\lambda_{g_0}}{\lambda_{g_0}K_p + \sigma^2}, \ldots, \frac{\lambda_{g_{r-1}}}{\lambda_{g_{r-1}}K_p + \sigma^2}, 0, \ldots, 0\right\}.\end{aligned} \tag{17}$$

Since our ultimate goal is to obtain MMSE estimator for the channel frequency response $\mathbf{H}$, from the invariance property of the MMSE estimator, it follows that if $\hat{\mathbf{g}}$ is the estimate of $\mathbf{g}$, then the corresponding estimate of $\mathbf{H}$ can be obtained for the ith OFDM block as

$$\hat{\mathbf{H}} = \mathcal{F}\boldsymbol{\Psi}\hat{\mathbf{g}}. \tag{18}$$

Thus, from (16) and (17), the truncated MMSE estimator of $\mathbf{g}$ requires $4Lr + 4LK_p + 2r$ real multiplications.

3.5. Performance analysis

We turn our attention to analytical performance results of the batch MMSE approach. We first consider the CRB and derive the closed-form expression for the random KL coefficients, and then exploit the performance of the MMSE channel estimator based on the evaluation of minimum Bayesian MSE.

3.5.1. Cramér-Rao bound for random KL coefficients

The mean squared estimation error for unbiased estimation of a nonrandom parameter has a lower bound, the *Cramér-Rao bound* (CRB), which defines the ultimate accuracy of unbiased estimation procedure. Suppose $\hat{\mathbf{g}}$ is an unbiased estimator of a vector of unknown parameters $\mathbf{g}$ (i.e., $E\{\hat{\mathbf{g}}\} = \mathbf{g}$) then the mean squared error matrix is lower bounded by the inverse of the Fisher information matrix (FIM):

$$E\{(\mathbf{g}-\hat{\mathbf{g}})(\mathbf{g}-\hat{\mathbf{g}})^{\dagger}\} \geq \mathbf{J}^{-1}(\mathbf{g}). \tag{19}$$

Since the estimation of unknown random parameters $\mathbf{g}$ via MMSE approach is considered in this paper, the modified FIM needs to be taken into account in the derivation of stochastic CRB [12]. Fortunately, the modified FIM can be obtained by a straightforward modification of (19) as

$$\mathbf{J}_M(\mathbf{g}) \triangleq \mathbf{J}(\mathbf{g}) + \mathbf{J}_P(\mathbf{g}), \tag{20}$$

where $\mathbf{J}_P(\mathbf{g})$ represents the *a priori* information.

Under the assumption that $\mathbf{g}$ and $\tilde{\boldsymbol{\eta}}$ are independent of each other and $\tilde{\boldsymbol{\eta}}$ is a zero mean, from [12] and (10), the conditional PDF is given by

$$p(\tilde{\mathbf{Y}}|\mathbf{g}) = \frac{1}{\pi^{K_p}\left|\mathbf{C}_{\tilde{\boldsymbol{\eta}}}\right|} \exp\left\{-(\tilde{\mathbf{Y}}-\mathbf{F}\boldsymbol{\Psi}\mathbf{g})^{\dagger}\mathbf{C}_{\tilde{\boldsymbol{\eta}}}^{-1}(\tilde{\mathbf{Y}}-\mathbf{F}\boldsymbol{\Psi}\mathbf{g})\right\} \tag{21}$$

from which the derivatives follow as

$$\begin{aligned}\frac{\partial \ln p(\tilde{\mathbf{Y}}|\mathbf{g})}{\partial \mathbf{g}^{T}} &= (\tilde{\mathbf{Y}}-\mathbf{F}\boldsymbol{\Psi}\mathbf{g})^{\dagger}\mathbf{C}_{\tilde{\boldsymbol{\eta}}}^{-1}\mathbf{F}\boldsymbol{\Psi},\\ \frac{\partial^2 \ln p(\tilde{\mathbf{Y}}|\mathbf{g})}{\partial \mathbf{g}^{*}\partial \mathbf{g}^{T}} &= -\boldsymbol{\Psi}^{\dagger}\mathbf{F}^{\dagger}\mathbf{C}_{\tilde{\boldsymbol{\eta}}}^{-1}\mathbf{F}\boldsymbol{\Psi},\end{aligned} \tag{22}$$

where the superscript $(\cdot)^*$ indicates the conjugation operation.

Using $\mathbf{C}_{\tilde{\boldsymbol{\eta}}} = \sigma^2\mathbf{I}_{K_p}$, $\boldsymbol{\Psi}^{\dagger}\boldsymbol{\Psi} = \mathbf{I}_L$, and $\mathbf{F}^{\dagger}\mathbf{F} = K_p\mathbf{I}_L$, and taking the expected value yield the following simple form:

$$\begin{aligned}\mathbf{J}(\mathbf{g}) &= -E\left[\frac{\partial^2 \ln p(\tilde{\mathbf{Y}}|\mathbf{g})}{\partial \mathbf{g}^{*}\partial \mathbf{g}^{T}}\right]\\ &= -E\left[-\frac{K_p}{\sigma^2}\mathbf{I}_L\right] = \frac{K_p}{\sigma^2}\mathbf{I}_L.\end{aligned} \tag{23}$$

The second term in (20) is easily obtained as follows. Consider the prior PDF of $\mathbf{g}$ as

$$p(\mathbf{g}) = \frac{1}{\pi^{L}\left|\boldsymbol{\Lambda}_{\mathbf{g}}\right|} \exp\left\{-\mathbf{g}^{\dagger}\boldsymbol{\Lambda}_{\mathbf{g}}^{-1}\mathbf{g}\right\}. \tag{24}$$

The respective derivatives are found as

$$\begin{aligned}\frac{\partial \ln p(\mathbf{g})}{\partial \mathbf{g}^{T}} &= -\mathbf{g}^{\dagger}\boldsymbol{\Lambda}_{\mathbf{g}}^{-1},\\ \frac{\partial^2 \ln p(\mathbf{g})}{\partial \mathbf{g}^{*}\partial \mathbf{g}^{T}} &= -\boldsymbol{\Lambda}_{\mathbf{g}}^{-1}.\end{aligned} \tag{25}$$

Upon taking the negative expectations, the second term in (20) becomes

$$\begin{aligned}\mathbf{J}_P(\mathbf{g}) &= -E\left[\frac{\partial^2 \ln p(\mathbf{g})}{\partial \mathbf{g}^{*}\partial \mathbf{g}^{T}}\right]\\ &= -E\left[-\boldsymbol{\Lambda}_{\mathbf{g}}^{-1}\right]\\ &= \boldsymbol{\Lambda}_{\mathbf{g}}^{-1}.\end{aligned} \tag{26}$$

Substituting (23) and (26) in (20) produces for the modified FIM the following:

$$\begin{aligned}\mathbf{J}_M(\mathbf{g}) &= \mathbf{J}(\mathbf{g}) + \mathbf{J}_P(\mathbf{g})\\ &= \frac{K_p}{\sigma^2}\mathbf{I}_L + \boldsymbol{\Lambda}_{\mathbf{g}}^{-1}\\ &= \frac{1}{\sigma^2}\left(K_p\mathbf{I}_L + \sigma^2\boldsymbol{\Lambda}_{\mathbf{g}}^{-1}\right)\\ &= \frac{1}{\sigma^2}\boldsymbol{\Gamma}^{-1}.\end{aligned} \tag{27}$$

Inverting the matrix $\mathbf{J}_M(\mathbf{g})$ yields

$$\mathrm{CRB}(\hat{\mathbf{g}}) = \mathbf{J}_M^{-1}(\mathbf{g}) = \sigma^2\boldsymbol{\Gamma}. \tag{28}$$

3.5.2. Bayesian MSE

For the MMSE estimator $\hat{\mathbf{g}}$, the error is

$$\boldsymbol{\epsilon} = \mathbf{g} - \hat{\mathbf{g}}. \tag{29}$$

Since the diagonal entries of the covariance matrix of the error represent the minimum Bayesian MSE, we now derive covariance matrix $\mathbf{C}_{\boldsymbol{\epsilon}}$ of the error vector. From *the performance of the MMSE estimator for the Bayesian linear model theorem* [11], the error covariance matrix is obtained as

$$\begin{aligned}\mathbf{C}_{\boldsymbol{\epsilon}} &= \left(\boldsymbol{\Lambda}_{\mathbf{g}}^{-1} + (\mathbf{F}\boldsymbol{\Psi})^{\dagger}\mathbf{C}_{\tilde{\boldsymbol{\eta}}}^{-1}(\mathbf{F}\boldsymbol{\Psi})\right)^{-1}\\ &= \sigma^2\left(K_p\mathbf{I}_L + \sigma^2\boldsymbol{\Lambda}_{\mathbf{g}}^{-1}\right)^{-1}\\ &= \sigma^2\boldsymbol{\Gamma}\end{aligned} \tag{30}$$

and then the minimum Bayesian MSE of the full rank estimator becomes (see Appendix A)

$$\begin{aligned}\mathbf{B}_{\mathrm{MSE}}(\hat{\mathbf{g}}) &= \frac{1}{L}\mathrm{tr}\left(\mathbf{C}_{\boldsymbol{\epsilon}}\right)\\ &= \frac{1}{L}\mathrm{tr}\left(\sigma^2\boldsymbol{\Gamma}\right) = \frac{1}{L}\sum_{i=0}^{L-1}\frac{\lambda_{g_i}}{1+K_p\lambda_{g_i}\,\mathrm{SNR}},\end{aligned} \tag{31}$$

where $\mathrm{SNR} = 1/\sigma^2$ and tr denotes trace operator on matrices.

Comparing (28) with (30), the error covariance matrix of the MMSE estimator coincides with the stochastic CRB of the random vector estimator. Thus, $\hat{\mathbf{g}}$ achieves the stochastic CRB.

As the details are given in Appendix A, $\mathbf{B}_{\mathrm{MSE}}(\hat{\mathbf{g}})$ given in (31) can also be computed for the truncated (low-rank) case as follows:

$$\mathbf{B}_{\mathrm{MSE}}(\hat{\mathbf{g}}_r) = \frac{1}{L}\sum_{i=0}^{r-1}\frac{\lambda_{g_i}}{1+K_p\lambda_{g_i}\,\mathrm{SNR}} + \frac{1}{L}\sum_{i=r}^{L-1}\lambda_{g_i}. \tag{32}$$

Notice that the second term in (32) is the sum of the powers in the KL transform coefficients not used in the truncated estimator. Thus, the truncated $\mathbf{B}_{\mathrm{MSE}}(\hat{\mathbf{g}}_r)$ can be lower bounded by $(1/L)\sum_{i=r}^{L-1}\lambda_{g_i}$ which will cause an irreducible error floor in the SER results.

3.6. Mismatch analysis

Once the true frequency-domain correlation, characterizing the channel statistics and the SNR, is known, the optimal channel estimator can be designed as indicated in Section 4.

However, in mobile wireless communications, the channel statistics depend on the particular environment, for example, indoor or outdoor, urban or suburban, and change with time. Hence, it is important to analyze the performance degradation due to a mismatch of the estimator to the channel statistics as well as the SNR, and to study the choice of the channel correlation and SNR for this estimator so that it is robust to variations in the channel statistics. As a performance measure, we use uncoded symbol error rate (SER) for QPSK signaling. The SER expression for this case is given in [13] as a function of the SNR and the average $\mathbf{B}_{\mathrm{MSE}}(\hat{\mathbf{g}})$ as follows:

$$\mathrm{SER}_{\mathrm{QPSK}} = \frac{3}{4} - \frac{\mu}{2} - \frac{\mu}{\pi}\arctan(\mu), \tag{33}$$

where

$$\mu = \frac{\Omega_g}{\sqrt{(\Omega_g + \mathbf{B}_{\mathrm{MSE}}(\hat{\mathbf{g}}))(1+2/\mathrm{SNR})}}, \tag{34}$$

and Ω_g represents the normalized variance of the channel gains ($\Omega_g = \sum_{i=0}^{L-1}\lambda_{g_i} = 1$) and $\mathrm{SNR} = 1/\sigma^2$. In practice, the true channel correlations and SNR are not known. If the MMSE channel estimator is designed to match the correlation of a multipath channel impulse response $\mathbf{C}_{\mathbf{h}}$ and SNR, but the true channel parameter $\widetilde{\mathbf{h}}$ has the correlation $\mathbf{C}_{\widetilde{\mathbf{h}}}$ and the true $\widetilde{\mathrm{SNR}}$, then average Bayesian MSE for the designed channel estimator is obtained as (see Appendices A and B)

(i) SNR mismatch:

$$\mathbf{B}_{\mathrm{MSE}}(\hat{\mathbf{g}}) = \frac{1}{L}\sum_{i=0}^{L-1}\frac{\lambda_{g_i}}{(1+K_p\lambda_{g_i}\,\mathrm{SNR})^2}\left[1+K_p\lambda_{g_i}\frac{\mathrm{SNR}^2}{\widetilde{\mathrm{SNR}}}\right]; \tag{35}$$

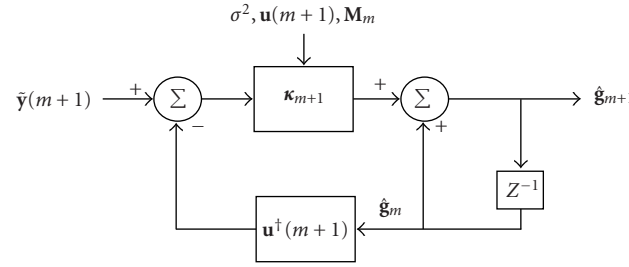

Figure 2: Block diagram of sequential MMSE estimator.

(ii) correlation mismatch:

$$\mathbf{B}_{\mathrm{MSE}}(\hat{\mathbf{g}}) = \frac{1}{L}\sum_{i=0}^{L-1}\frac{\widetilde{\lambda}_{g_i} + K_p\,\mathrm{SNR}\,\lambda_{g_i}(\widetilde{\lambda}_{g_i} + \lambda_{g_i} - 2\beta_i)}{1+K_p\,\mathrm{SNR}\,\lambda_{g_i}}, \tag{36}$$

where $\widetilde{\lambda}_{g_i}$ is the ith diagonal element of $\boldsymbol{\Lambda}_{\widetilde{\mathbf{g}}} = \boldsymbol{\Psi}^\dagger\mathbf{C}_{\widetilde{\mathbf{h}}}\boldsymbol{\Psi}$, and β_i is ith diagonal element of the real part of the cross-correlation matrix between $\widetilde{\mathbf{g}}$ and $\mathbf{g}$.

4. MMSE ESTIMATION OF KL COEFFICIENTS: SEQUENTIAL APPROACH

We now turn our attention to the derivation of the sequential MMSE algorithm with simple structure. The sequential MMSE approach is proposed in this paper to follow the channel variations by exploiting only channel correlations in frequency. The block diagram for this is shown in Figure 2.

To begin with the algebraic derivation, we use (10) to write mth component of $\widetilde{\mathbf{Y}}$ as

$$\widetilde{\mathbf{Y}}[m] = \mathbf{u}^\dagger(m)\mathbf{g} + \widetilde{\boldsymbol{\eta}}[m], \tag{37}$$

where $\mathbf{u}^\dagger(m)$ is the mth row of $\mathbf{F}\boldsymbol{\Psi}$ and $\widetilde{\boldsymbol{\eta}}[m]$ is the mth element of the noise vector $\widetilde{\boldsymbol{\eta}}$.

If an MMSE estimator of $\widetilde{\mathbf{Y}}[m+1]$ can be found based on $\widetilde{\mathbf{Y}}[m]$, denoted by $\widehat{\widetilde{\mathbf{Y}}}_{m+1|m}$, the prediction error $f_{m+1} = \widetilde{\mathbf{Y}}[m+1] - \widehat{\widetilde{\mathbf{Y}}}_{m+1|m}$ will be orthogonal to $\widetilde{\mathbf{Y}}[m]$. We can therefore project $\mathbf{g}$ onto each vector separately and add the results, so that

$$\begin{aligned}\hat{\mathbf{g}}_{m+1} &= \hat{\mathbf{g}}_m + \boldsymbol{\kappa}_{m+1}f_{m+1}\\ &= \hat{\mathbf{g}}_m + \boldsymbol{\kappa}_{m+1}(\widetilde{\mathbf{Y}}[m+1] - \mathbf{u}^\dagger(m+1)\hat{\mathbf{g}}_m),\end{aligned} \tag{38}$$

where $\hat{\mathbf{g}}_{m+1}$ is the $(m+1)$th estimate of $\mathbf{g}$, and $\boldsymbol{\kappa}_{m+1}$ is the gain factor given as

$$\boldsymbol{\kappa}_{m+1} = \frac{\mathbf{M}_m\mathbf{u}(m+1)}{\mathbf{u}^\dagger(m+1)\mathbf{M}_m\mathbf{u}(m+1)+\sigma^2}. \tag{39}$$

It can be seen that $\mathbf{M}_m = E[(\mathbf{g}-\hat{\mathbf{g}}_m)\ (\mathbf{g}-\hat{\mathbf{g}}_m)^\dagger]$ is needed in (39), hence update equation for the minimum MSE matrix should also be given. If we substitute (38) in $\mathbf{M}_{m+1} = E[(\mathbf{g}-\hat{\mathbf{g}}_{m+1})\ (\mathbf{g}-\hat{\mathbf{g}}_{m+1})^\dagger]$, we obtain an update equation

for $\mathbf{M}_{m+1}$ as

$$\mathbf{M}_{m+1} = [\mathbf{I} - \boldsymbol{\kappa}_{m+1}\mathbf{u}^{\dagger}(m+1)]\mathbf{M}_m. \tag{40}$$

Based on these results, the steps of the sequential MMSE estimator for $\mathbf{g}$ can be summarized as follows.

Initialization. Set the parameters to some initial value $\hat{\mathbf{g}}_0 = \mathbf{0}, \mathbf{M}_0 = \boldsymbol{\Lambda}_{\mathbf{g}}$.

(1) Compute the gain $\boldsymbol{\kappa}_{m+1}$ from (39).
(2) Update the estimate of $\mathbf{g}$ from (38).
(3) Update the minimum MSE matrix from (40).
(4) Repeat step (1)–step (3) until $m = K_p - 1$.

Some remarks and observations are now in order.

(i) No matrix inversions are required.
(ii) Since the MMSE estimator (11) requires $\mathbf{F}^{\dagger}\mathbf{F}$ to be equal to $K_p\mathbf{I}$ which is satisfied only when $\Delta = K/K_p$ is an integer, however, the sequential version of (11) works as long as $\Delta \leq K/L$.

We now analyze the complexity of the sequential MMSE algorithm. It follows from (39) in step (1) that one needs $4L^2 + 5L$ real multiplications to compute the gain. Similarly, from (38) in step (2), it requires $5L$ real multiplications for the estimator update. Finally, in step (3), we need $8L^2$ real multiplications for the MMSE matrix update. Therefore, the total sequential MMSE algorithm requires $12L^2 + 10L$ real multiplications for one iteration.

4.1. Performance analysis

We turn our attention now to the performance analysis of the adaptive algorithm. We will try to evaluate its convergence properties in terms of mean square error.

From (39) and (40), we conclude that

$$\begin{aligned}\boldsymbol{\kappa}_{m+1}\sigma^2 &= (\mathbf{I} - \boldsymbol{\kappa}_{m+1}\mathbf{u}^{\dagger}(m+1))\mathbf{M}_m\mathbf{u}(m+1)\\ &= \mathbf{M}_{m+1}\mathbf{u}(m+1).\end{aligned} \tag{41}$$

Substituting (41) in (39), we have

$$\left(\mathbf{M}_{m+1} - \frac{\sigma^2}{\mathbf{u}^{\dagger}(m+1)\mathbf{M}_m\mathbf{u}(m+1) + \sigma^2}\mathbf{M}_m\right)\mathbf{u}(m+1) = \mathbf{0}_{L\times 1}. \tag{42}$$

Based on (42), the following recursion is obtained:

$$\begin{aligned}\mathbf{M}_{m+1} &= \frac{\sigma^2}{\mathbf{u}^{\dagger}(m+1)\mathbf{M}_m\mathbf{u}(m+1) + \sigma^2}\mathbf{M}_m\\ &= \delta_{m+1|m}\mathbf{M}_m.\end{aligned} \tag{43}$$

Due to positive definite property of error covariance matrix $\mathbf{M}_m$, it follows that $\mathbf{u}^{\dagger}(m+1)\mathbf{M}_m\mathbf{u}(m+1) > 0$. As a result, $0 < \delta_{m+1|m} < 1$.

Define average MSE at the mth step as $\mathrm{MSE}_m = (1/L)\,\mathrm{tr}(\mathbf{M}_m)$, then it follows from (43) that

$$\mathrm{MSE}_{m+1} = \delta_{m+1|m}\,\mathrm{MSE}_m\,. \tag{44}$$

Thus, we observe that as $m \to \infty$, $\mathrm{MSE}_m \to 0$ which means that $\hat{\mathbf{g}}_m$ converges to $\mathbf{g}$ in the mean square.

5. SIMULATIONS

In this section, the merits of our channel estimators are illustrated through simulations. We choose average mean square error (MSE) and symbol error rate (SER) as our figure of merits. We consider the fading multipath channel with L paths given by (45) with an exponentially decaying power delay profile $\theta(\tau_l) = Ce^{-\tau_l/\tau_{\mathrm{RMS}}}$ with delays τ_l that are uniformly and independently distributed over the length L_{CP}. Note that $\mathbf{h}$ is chosen as complex Gaussian leading to a Rayleigh fading channel with root mean square (RMS) width τ_{RMS} and normalizing constant C. In [3], it is shown that the normalized exponential discrete channel correlation for different subcarriers is

$$r_f(k) = \frac{1 - \exp\left(-L(1/\tau_{\mathrm{RMS}} + 2\pi jk/K)\right)}{\tau_{\mathrm{RMS}}\left(1 - \exp\left(-L/\tau_{\mathrm{RMS}}\right)\right)\left(1/\tau_{\mathrm{RMS}} + 2\pi jk/K\right)}. \tag{45}$$

The scenario for our simulation study consists of a wireless QPSK-OFDM system employing the pulse shape as a unit-energy Nyquist-root raised-cosine shape with rolloff $\alpha = 0.2$, with a symbol period (T_s) of 0.120 microsecond, corresponding to an uncoded symbol rate of 8.33 Mbps. Transmission bandwidth (5 MHz) is divided into 1024 tones. We assume that the fading multipath channel has $L = 40$ paths with an exponentially decaying power delay profile (45) with $\tau_{\mathrm{RMS}} = 5$ sample (0.6 microsecond) long.

5.1. Batch MMSE approach

A QPSK-OFDM sequence passes through channel taps and is corrupted by AWGN (0 dB, 5 dB, 10 dB, 15 dB, 20 dB, 25 dB, and 30 dB, respectively). We use a pilot symbol for every twenty ($\Delta = 20$) symbols. The MSE at each SNR point is averaged over 1000 realizations. We compare the experimental MSE performance and its theoretical Bayesian MSE of the proposed full-rank MMSE estimator with maximum-likelihood (ML) estimator and its corresponding Cramér-Rao bound (CRB). Figure 3 confirms that MMSE estimator performs better than ML estimator at low SNR. However, the 2 approaches have comparable performance at high SNRs. To observe the performance, we also present the MMSE and ML estimated channel SER results together with theoretical SER in Figure 4. Due to the fact that spaces between the pilot symbols are not chosen as a factor of the number of subcarriers, an error floor is observed in Figures 3 and 4. In the case of choosing the pilot space as a factor of number of subcarriers, the error floor vanishes because of the fact that the orthogonality condition between the subcarriers at pilot locations is satisfied. In other words, the curves labeled as simulation results for MMSE estimator and ML estimator fit to the theoretical curve at high SNRs. It also shows that the MMSE estimated channel SER results are better than ML estimated channel SER especially at low SNRs.

5.1.1. SNR design mismatch

In order to evaluate the performance of the proposed full-rank MMSE estimator to mismatch only in SNR design, the

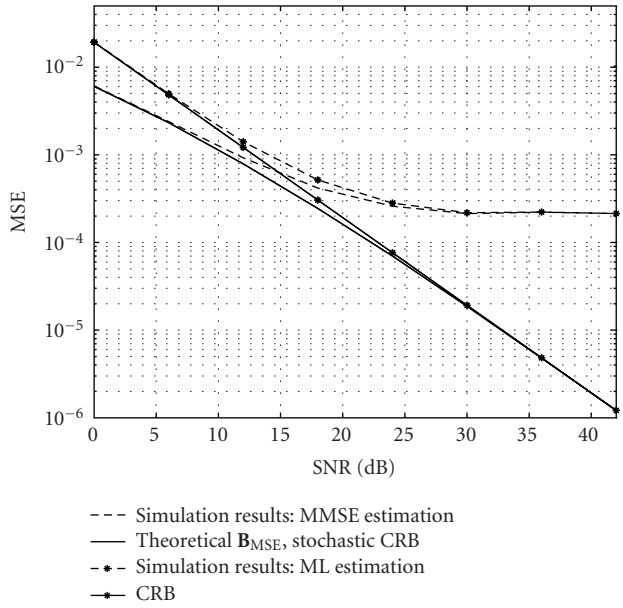

Figure 3: Performance of proposed MMSE and MLE together with $\mathbf{B}_{\mathrm{MSE}}$ and CRB.

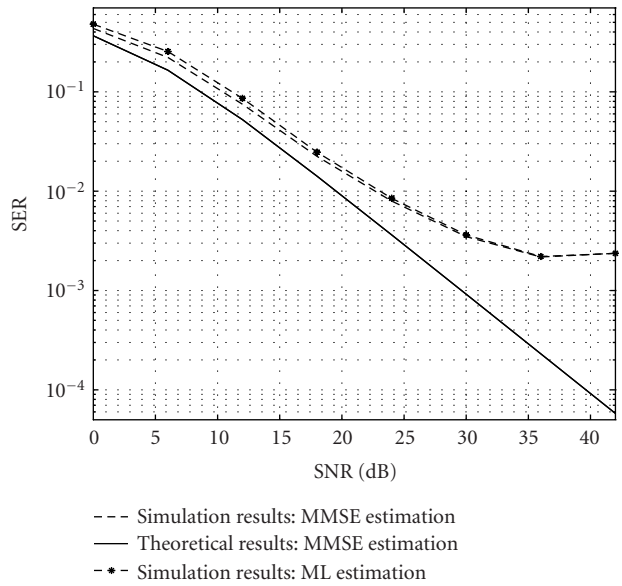

Figure 4: Symbol error rate results.

estimator is tested when SNRs of 10 and 30 dB are used in the design. The SER curves for a design SNR of 10, 30 dB are shown in Figure 5. The performance of the MMSE estimator for high SNR (30 dB) design is better than low SNR (10 dB) design across a range of SNR values (0–30 dB). This results confirm that channel estimation error is concealed in noise for low SNR whereas it tends to dominate for high SNR. Thus, the system performance degrades especially for low SNR design.

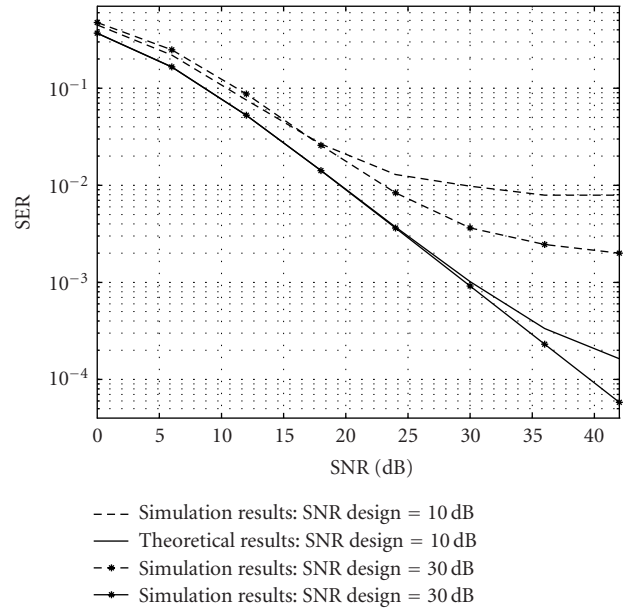

Figure 5: Effects of SNR design mismatch on SER.

5.1.2. Correlation mismatch

To further analyze full-rank MMSE estimator's performance, we need to study sensitivity of the estimator to design errors, that is, correlation mismatch. We therefore designed the estimator for a uniform channel correlation which gives the worst MSE performance among all channels [3, 5] and evaluated it for an exponentially decaying power delay profile. The uniform channel correlation between the attenuations can be obtained by letting $\tau_{\mathrm{RMS}} \to \infty$ in (45), resulting in

$$r_f(k) = \frac{1 - \exp(2\pi jLk/K)}{2\pi jk/K}. \tag{46}$$

Figures 6 and 7 demonstrate the estimator's sensitivity to the channel statistics in terms of average MSE and SER performance measures, respectively. As it can be seen from Figures 6 and 7, only small performance loss is observed for low SNRs when the estimator is designed for mismatched channel statistics. This justifies the result that a design for worst correlation is robust to mismatch.

5.1.3. Performance of the truncated estimator

The truncated estimator performance is also studied as a function of the number of KL coefficients. Figure 8 presents the MSE result of the truncated MMSE estimator for SNR = 10, 20, and 30 dB. If only a few expansion coefficients are employed to reduce the complexity of the proposed estimator, then the MSE between channel parameters becomes large. However, if the number of parameters in the expansion is increased, the irreducible error floor still occurs.

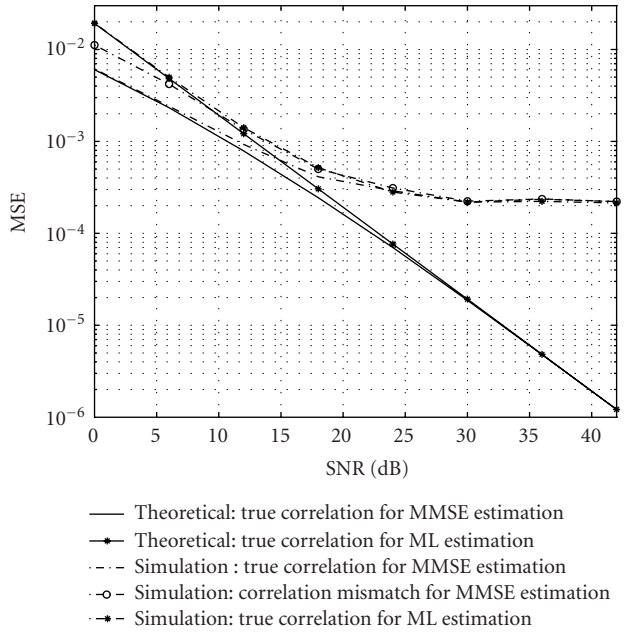

Figure 6: Effects of correlation mismatch on MSE.

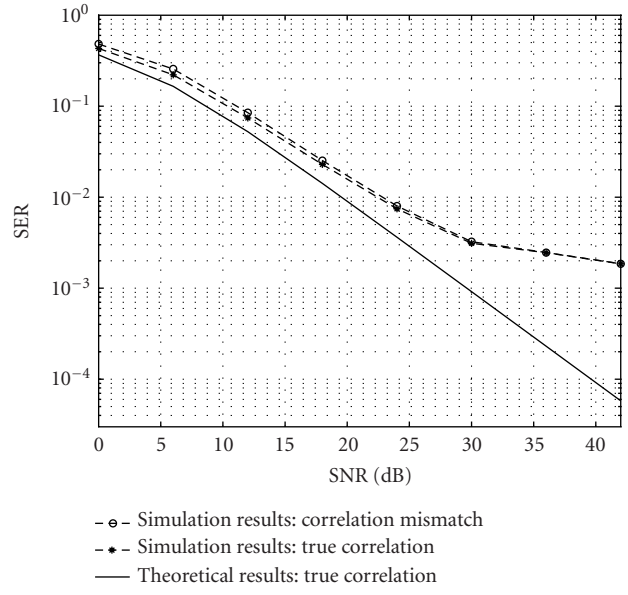

Figure 7: Effects of correlation mismatch on SER.

5.2. Sequential MMSE approach

The MSE results of the sequential full-rank MMSE algorithm are obtained and presented as shown in Figure 9. In order to better evaluate the performance of the proposed sequential MMSE estimation algorithm, we compare it with previously developed least mean square (LMS) and recursive least squares (RLS) algorithms. It can be seen from simulations that recursive MMSE estimator yields better performance than LMS and RLS approaches and achieves Bayesian MSE especially for low SNR.

For the convergence of the proposed adaptive algorithm, MSE versus iteration is plotted for SNR $= 10, 20, 30$, and 40 dB in Figure 10. As expected, the proposed sequential algorithm converges faster for high SNR values.

Finally, we wish to evaluate the performance of the algorithm for different values of pilot spacing 10, 20, 30, 40, and 50 by plotting the MSEs and SERs with respect to SNR in Figures 11 and 12, respectively. For the values pilot spacing Δ larger than K/L, the SER and MSE performances decrease as Δ increases.

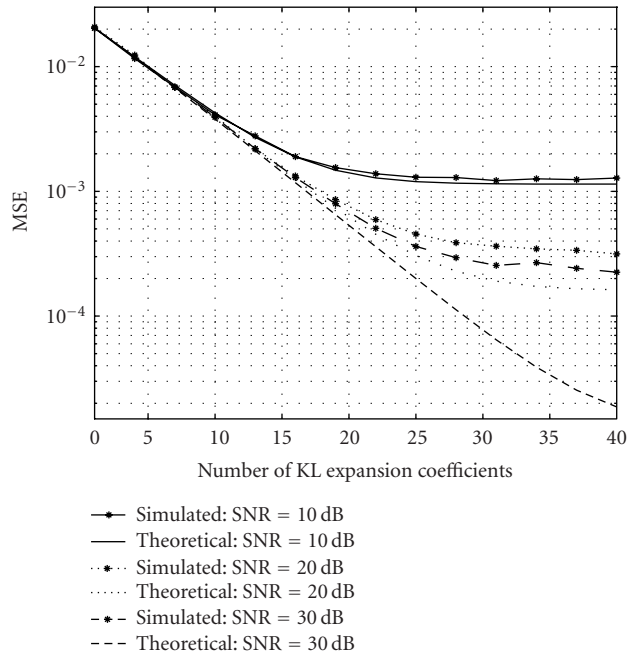

Figure 8: MSE as a function of KL expansion coefficients.

6. CONCLUSION

We consider the design of low-complexity MMSE channel estimators for OFDM systems in unknown wireless dispersive fading channels. We first derive the batch MMSE estimator based on the stochastic orthogonal expansion representation of the channel via KL transform. Based on such representation, we show that no matrix inversion is needed in the MMSE algorithm. Therefore, the computational cost for implementing the proposed MMSE estimator is low and computation is numerically stable. Moreover, the performance of our proposed batch method was first studied through the derivation of stochastic CRB for Bayesian approach. Since the actual channel statistics and SNR may vary within OFDM block, we have also analyzed the effect of modelling mismatch on the estimator performance and shown both analytically and through simulations that the performance degradation due to such mismatch is negligible for low SNR values. The MMSE estimator is then extended to sequential implementation which enjoys the elegance of the simple structure and fast convergence.

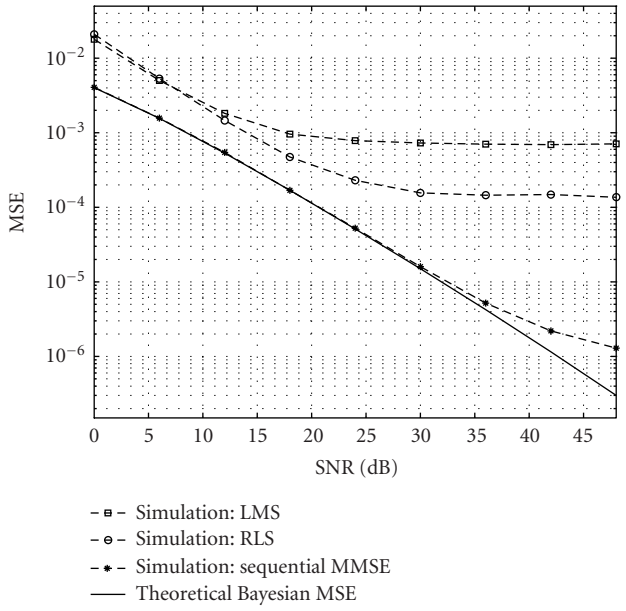

Figure 9: Sequential MMSE performance.

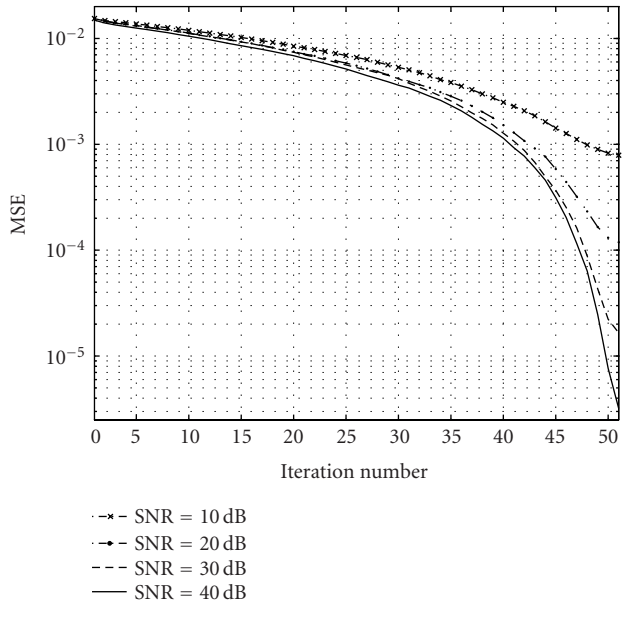

Figure 10: Convergence of the sequential MMSE estimator.

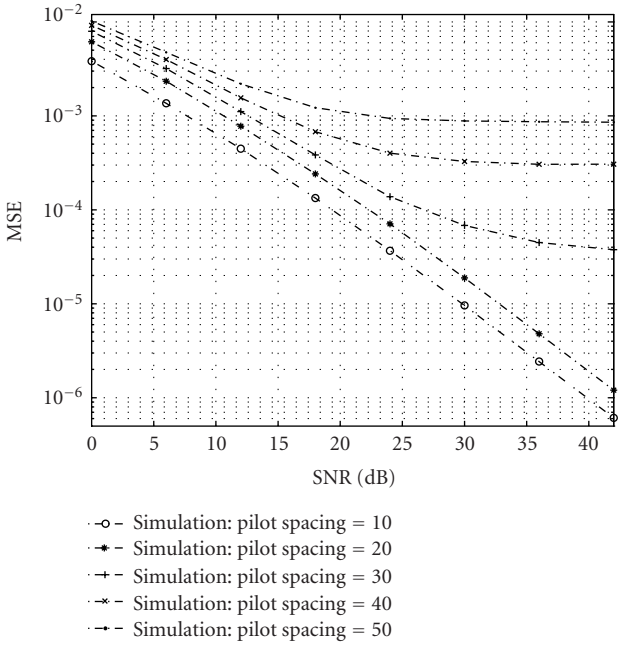

Figure 11: Performance of the sequential MMSE for different pilot spacings.

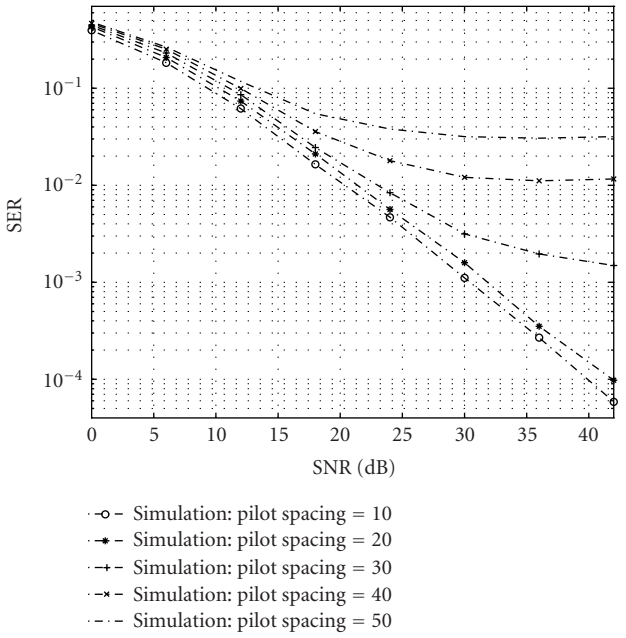

Figure 12: Symbol error rate of the sequential MMSE for different pilot spacings.

APPENDICES

A. BAYESIAN MSE FOR TRUNCATED MMSE KL ESTIMATOR UNDER SNR MISMATCH

Substituting (10) in (16), the truncated MMSE KL estimator now becomes

$$\hat{\mathbf{g}}_r = K_p \boldsymbol{\Gamma}_r \mathbf{g} + \boldsymbol{\Gamma}_r \boldsymbol{\Psi}^{\dagger} \mathbf{F}^{\dagger} \tilde{\boldsymbol{\eta}}. \tag{A.1}$$

The estimation error

$$\begin{aligned} \hat{\boldsymbol{\epsilon}}_r &= \mathbf{g} - \hat{\mathbf{g}}_r \\ &= \mathbf{g} - \left(K_p \boldsymbol{\Gamma}_r \mathbf{g} + \boldsymbol{\Gamma}_r \boldsymbol{\Psi}^{\dagger} \mathbf{F}^{\dagger} \tilde{\boldsymbol{\eta}}\right) \\ &= \left(\mathbf{I}_L - K_p \boldsymbol{\Gamma}_r\right) \mathbf{g} - \boldsymbol{\Gamma}_r \boldsymbol{\Psi}^{\dagger} \mathbf{F}^{\dagger} \tilde{\boldsymbol{\eta}} \end{aligned} \tag{A.2}$$

and then the average Bayesian MSE is

$$\begin{aligned}
\mathbf{B}_{\mathrm{MSE}}(\hat{\mathbf{g}}_r) &= \frac{1}{L}\operatorname{tr}\left(\mathbf{C}_{\hat{\epsilon}_r}\right)\\
&= \frac{1}{L}\operatorname{tr}\left(\mathbf{\Lambda}_{\mathbf{g}}(\mathbf{I}_L - K_p\mathbf{\Gamma}_r)^2 + K_p\tilde{\sigma}^2\mathbf{\Gamma}_r^2\right)\\
&= \frac{1}{L}\sum_{i=0}^{r-1}\left[\lambda_{g_i}\left(1 - K_p\frac{\lambda_{g_i}}{\lambda_{g_i}K_p+\sigma^2}\right)^2\right.\\
&\qquad\left. + K_p\tilde{\sigma}^2\left(\frac{\lambda_{g_i}}{\lambda_{g_i}K_p+\sigma^2}\right)^2\right] + \frac{1}{L}\sum_{i=r}^{L-1}\lambda_{g_i}\\
&= \frac{1}{L}\sum_{i=0}^{r-1}\lambda_{g_i}\frac{\tilde{\sigma}^2K_p\lambda_{g_i}+\sigma^4}{\left(K_p\lambda_{g_i}+\sigma^2\right)^2} + \frac{1}{L}\sum_{i=r}^{L-1}\lambda_{g_i}\\
&\qquad \text{where } \sigma^2 = \frac{1}{\mathrm{SNR}},\ \tilde{\sigma}^2 = \frac{1}{\widetilde{\mathrm{SNR}}}\\
&= \frac{1}{L}\sum_{i=0}^{r-1}\frac{\lambda_{g_i}}{\left(1+K_p\lambda_{g_i}\,\mathrm{SNR}\right)^2}\left[1 + K_p\lambda_{g_i}\frac{\mathrm{SNR}^2}{\widetilde{\mathrm{SNR}}}\right]\\
&\quad + \frac{1}{L}\sum_{i=r}^{L-1}\lambda_{g_i}.
\end{aligned} \tag{A.3}$$

Based on the result obtained in (A.3), Bayesian estimator performance can be further elaborated for the following scenarios.

(i) By taking $\widetilde{\mathrm{SNR}} = \mathrm{SNR}$, the performance result for the case of no SNR mismatch is

$$\mathbf{B}_{\mathrm{MSE}}(\hat{\mathbf{g}}_r) = \frac{1}{L}\sum_{i=0}^{r-1}\frac{\lambda_{g_i}}{1+K_p\lambda_{g_i}\,\mathrm{SNR}} + \frac{1}{L}\sum_{i=r}^{L-1}\lambda_{g_i}. \tag{A.4}$$

(ii) As $r \to L$ in (A.3), $\mathbf{B}_{\mathrm{MSE}}(\hat{\mathbf{g}})$ under SNR mismatch results in the following Bayesian MSE:

$$\mathbf{B}_{\mathrm{MSE}}(\hat{\mathbf{g}}) = \frac{1}{L}\sum_{i=0}^{L-1}\frac{\lambda_{g_i}}{\left(1+K_p\lambda_{g_i}\,\mathrm{SNR}\right)^2}\left[1 + K_p\lambda_{g_i}\frac{\mathrm{SNR}^2}{\widetilde{\mathrm{SNR}}}\right]. \tag{A.5}$$

(iii) Finally, the Bayesian MSE in the case of no SNR mismatch can also be obtained as

$$\mathbf{B}_{\mathrm{MSE}}(\hat{\mathbf{g}}) = \frac{1}{L}\sum_{i=0}^{L-1}\frac{\lambda_{g_i}}{1+K_p\lambda_{g_i}\,\mathrm{SNR}}. \tag{A.6}$$

B. BAYESIAN MSE FOR TRUNCATED MMSE KL ESTIMATOR UNDER CORRELATION MISMATCH

In this appendix, we derive the Bayesian MSE of the truncated MMSE KL estimator under correlation mismatch. Although the real multipath channel $\tilde{\mathbf{h}}$ has the expansion correlation $\mathbf{C}_{\tilde{\mathbf{h}}}$, we designed the estimator for the multipath channel $\mathbf{h} = \mathbf{\Psi}\mathbf{g}$ with correlation $\mathbf{C}_{\mathbf{h}}$. To evaluate the estimation error $\tilde{\mathbf{g}} - \hat{\mathbf{g}}_r$ in the same space, we expand $\tilde{\mathbf{h}}$ onto the eigenspace of $\mathbf{h}$ as $\tilde{\mathbf{h}} = \mathbf{\Psi}\tilde{\mathbf{g}}$ resulting in correlated expansion coefficients.

For the real channel, data model in (10) can be rewritten as

$$\tilde{\mathbf{Y}} = \mathbf{F}\mathbf{\Psi}\tilde{\mathbf{g}} + \tilde{\boldsymbol{\eta}} \tag{B.1}$$

and substituting in (16), the truncated MMSE KL estimator now becomes

$$\hat{\mathbf{g}}_r = K_p\mathbf{\Gamma}_r\mathbf{g} + \mathbf{\Gamma}_r\mathbf{\Psi}^\dagger\mathbf{F}^\dagger\tilde{\boldsymbol{\eta}}. \tag{B.2}$$

For the truncated MMSE estimator, the error is

$$\begin{aligned}
\hat{\boldsymbol{\epsilon}}_r &= \tilde{\mathbf{g}} - \hat{\mathbf{g}}_r\\
&= \tilde{\mathbf{g}} - K_p\mathbf{\Gamma}_r\mathbf{g} - \mathbf{\Gamma}_r\mathbf{\Psi}^\dagger\mathbf{F}^\dagger\tilde{\boldsymbol{\eta}}.
\end{aligned} \tag{B.3}$$

As a result, the average Bayesian MSE is

$$\begin{aligned}
\mathbf{B}_{\mathrm{MSE}}(\hat{\mathbf{g}}_r) &= \frac{1}{L}\operatorname{tr}\left(\mathbf{C}_{\hat{\epsilon}_r}\right)\\
&= \frac{1}{L}\operatorname{tr}\left(\mathbf{\Lambda}_{\tilde{\mathbf{g}}} + K_p^2\mathbf{\Gamma}_r^2\mathbf{\Lambda}_{\mathbf{g}} + \sigma^2K_p\mathbf{\Gamma}_r^2 - 2K_p\mathbf{\Gamma}_r\boldsymbol{\beta}\right)\\
&= \frac{1}{L}\sum_{i=0}^{r-1}\left[\tilde{\lambda}_{g_i} + \frac{K_p\lambda_{g_i}\left(\lambda_{g_i}-2\beta_i\right)}{K_p\lambda_{g_i}+\sigma^2}\right]\\
&\quad + \frac{1}{L}\sum_{i=r}^{L-1}\tilde{\lambda}_{g_i}, \quad \sigma^2 = \frac{1}{\mathrm{SNR}}\\
&= \frac{1}{L}\sum_{i=0}^{r-1}\left[\tilde{\lambda}_{g_i} + \frac{K_p\,\mathrm{SNR}\,\lambda_{g_i}\left(\lambda_{g_i}-2\beta_i\right)}{1+K_p\,\mathrm{SNR}\,\lambda_{g_i}}\right] + \frac{1}{L}\sum_{i=r}^{L-1}\tilde{\lambda}_{g_i}\\
&= \frac{1}{L}\sum_{i=0}^{r-1}\frac{\tilde{\lambda}_{g_i} + K_p\,\mathrm{SNR}\,\lambda_{g_i}\left(\tilde{\lambda}_{g_i}+\lambda_{g_i}-2\beta_i\right)}{1+K_p\,\mathrm{SNR}\,\lambda_{g_i}}\\
&\quad + \frac{1}{L}\sum_{i=r}^{L-1}\tilde{\lambda}_{g_i},
\end{aligned} \tag{B.4}$$

where $\boldsymbol{\beta}$ is the real part of $E[\tilde{\mathbf{g}}\mathbf{g}^\dagger]$ and β_i's are the diagonal elements of $\boldsymbol{\beta}$. With this result, we will now highlight some special cases.

(i) Letting $\beta_i = \lambda_{g_i} = \tilde{\lambda}_{g_i}$ in (B.4) for the case of no mismatch in the correlation of KL expansion coefficients, the truncated Bayesian MSE is identical to that obtained in (A.4).

(ii) As $r \to L$ in (B.4), Bayesian MSE under correlation mismatch is obtained to yield

$$\mathbf{B}_{\mathrm{MSE}}(\hat{\mathbf{g}}) = \frac{1}{L}\sum_{i=0}^{L-1}\frac{\tilde{\lambda}_{g_i} + K_p\,\mathrm{SNR}\,\lambda_{g_i}\left(\tilde{\lambda}_{g_i}+\lambda_{g_i}-2\beta_i\right)}{1+K_p\,\mathrm{SNR}\,\lambda_{g_i}}. \tag{B.5}$$

(iii) Under no correlation mismatch in (B.5) where $\beta_i = \lambda_{g_i} = \tilde{\lambda}_{g_i}$, Bayesian MSE obtained from (B.5) is identical to that in (A.6).

(iv) Also note that as SNR $\to \infty$, (B.4) reduces to MSE$(\tilde{\mathbf{g}} - \mathbf{g}_r)$.

ACKNOWLEDGMENTS

This paper has been produced as part of the NEWCOM Network of Excellence, a project funded by the European Commission's 6th Framework Programme. This work was supported by the Research Fund of the University of Istanbul, Project numbers UDP-362/04082004 and 220/29042004. Part of the results of this paper was presented at the Sixth Baiona Workshop on Signal Processing in Communications, Baiona, Spain, September 8–10, 2003.

REFERENCES

[1] R. Van Nee and R. Prasad, *OFDM for Wireless Multimedia Communications*, Artech House Publishers, Boston, Mass, USA, 2000.

[2] H. Sari, G. Karam, and I. Jeanclaude, "Transmission techniques for digital terrestrial TV broadcasting," *IEEE Commun. Mag.*, vol. 33, no. 2, pp. 100–109, 1995.

[3] O. Edfors, M. Sandell, J.-J. van de Beek, S. K. Wilson, and P. O. Borjesson, "OFDM channel estimation by singular value decomposition," *IEEE Trans. Commun.*, vol. 46, no. 7, pp. 931–939, 1998.

[4] M. Morelli and U. Mengali, "A comparison of pilot-aided channel estimation methods for OFDM systems," *IEEE Trans. Signal Processing*, vol. 49, no. 12, pp. 3065–3073, 2001.

[5] Y. Li, L. J. Cimini, and N. R. Sollenberger, "Robust channel estimation for OFDM systems with rapid dispersive fading channels," *IEEE Trans. Commun.*, vol. 46, no. 7, pp. 902–915, 1998.

[6] P. Schniter, "Low-complexity estimation of doubly-selective channels," in *Proc. IEEE Workshop on Signal Processing Advances in Wireless Communications (SPAWC '03)*, pp. 200–204, Rome, Italy, June 2003.

[7] E. Biglieri, J. Proakis, and S. Shamai, "Fading channels: information-theoretic and communications aspects," *IEEE Trans. Inform. Theory*, vol. 44, no. 6, pp. 2619–2692, 1998.

[8] W. C. Jakes Jr., *Microwave Mobile Communications*, John Wiley & Sons, New York, NY, USA, 1974.

[9] K. W. Yip and T.-S. Ng, "Karhunen-Loeve expansion of the WSSUS channel output and its application to efficient simulation," *IEEE J. Select. Areas Commun.*, vol. 15, no. 4, pp. 640–646, 1997.

[10] M. Siala and D. Duponteil, "Maximum a posteriori multipath fading channel estimation for CDMA systems," in *IEEE 49th Vehicular Technology Conference (VTC '99)*, vol. 2, pp. 1121–1125, Houston, Tex, USA, May 1999.

[11] S. M. Kay, *Fundamentals of Statistical Signal Processing. Estimation Theory*, Prentice-Hall, Englewood Cliffs, NJ, USA, 1993.

[12] H. L. Van Trees, *Detection, Estimation, and Modulation Theory, Part I*, Wiley-Interscience, New York, NY, USA, 2001.

[13] J. Proakis, *Digital Communications*, McGraw-Hill, New York, NY, USA, 1983.

Habib Şenol received the B.S. and M.S. degrees from the University of Istanbul in 1993 and in 1999, respectively. He is currently a Ph.D. student in the Department of Electronics Engineering, IŞik University. From 1996 to 1999, he was a Research Assistant at the University of Istanbul. In 1999, as a Lecturer, he joined the faculty of the Department of Computer Engineering, Kadir Has University. His general research interests cover communication theory, estimation theory, statistical signal processing, and information theory. His current research activities are focused on wireless communication concepts with specific attention to channel estimation algorithms for multicarrier (OFDM) systems.

Hakan A. Çırpan received the B.S. degree in 1989 from Uludag University, Bursa, Turkey, the M.S. degree in 1992 from Istanbul University, Istanbul, Turkey, and the Ph.D. degree in 1997 from the Stevens Institute of Technology, Hoboken, New Jersey, USA, all in electrical engineering. From 1995 to 1997, he was a Research Assistant at the Stevens Institute of Technology, working on signal processing algorithms for wireless communication systems. In 1997, he joined the faculty of the Department of Electrical-Electronics Engineering, Istanbul University. His general research interests cover wireless communications, statistical signal and array processing, system identification, and estimation theory. His current research activities are focused on signal processing and communication concepts with specific attention to channel estimation and equalization algorithms for space-time coding and multicarrier (OFDM) systems. Dr. Çırpan received Peskin Award from Stevens Institute of Technology as well as Professor Nazim Terzioglu Award from the Research Fund of The University of Istanbul. He is a Member of IEEE and Member of Sigma Xi.

Erdal Panayırcı received the Diploma Engineering degree in electrical engineering from Istanbul Technical University, Istanbul, Turkey, in 1964, and the Ph.D. degree in electrical engineering and system science from Michigan State University, East Lansing Michigan, USA, in 1970. Between 1970–2000, he was with the Faculty of Electrical and Electronics Engineering at the Istanbul Technical University, where he was a Professor and Head of the Telecommunications Chair. Currently, he is a Professor and Head of the Electronics Engineering Department at IŞIK University, Istanbul, Turkey. He is engaged in research and teaching in digital communications and wireless systems, equalization and channel estimation in multicarrier (OFDM) communication systems, and efficient modulation and coding techniques (TCM and turbo coding). He spent two years (1979–1981) with the Department of Computer Science, Michigan State University, as a Fulbright-Hays Fellow and a NATO Senior Scientist. Between 1983-1986 he served as a NATO Advisory Committee Member for the Special Panel on Sensory Systems for Robotic Control. From August 1990 to December 1991, he was with the Center for Communications and Signal Processing, New Jersey Institute of Technology, as a Visiting Professor, and took part in the research project on interference cancellation by array processing. Between 1998–2000, he was a Visiting Professor in the Department of Electrical Engineering, Texas A&M University, and took part in research on developing efficient synchronization algorithms for OFDM systems. Between 1995–1999, Professor Panayırcı was an Editor for the IEEE Transactions on Communications in the fields of synchronization and equalizations. He is a Fellow of the IEEE and Member of Sigma Xi.